

See discussions, stats, and author profiles for this publication at: <https://www.researchgate.net/publication/371561795>

Thermodynamic analysis of absorption refrigeration cycles by parabolic trough collectors

Article in *Physics of Fluids* · June 2023

DOI: 10.1063/5.0153839

CITATIONS

0

READS

113

8 authors, including:



Abdullah Albaker
University of Hail

34 PUBLICATIONS 131 CITATIONS

SEE PROFILE










Reza Alayi
Islamic Azad University of Germi branch

101 PUBLICATIONS 877 CITATIONS

SEE PROFILE

RESEARCH ARTICLE | JUNE 13 2023

Thermodynamic analysis of absorption refrigeration cycles by parabolic trough collectors

Abdullah Albaker ; Nestor Cuba Carbajal ; Manuel Octavio Fernández Athó;
Anderson Nuñez Fernandez ; Maria Del Carmen Delgado Laime; Ani Mary Borda Echavarría;
Reza Alayi  ; Morteza Aladdin  



Physics of Fluids 35, 067118 (2023)
<https://doi.org/10.1063/5.0153839>

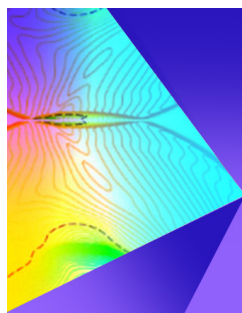


View
Online



Export
Citation

CrossMark



Physics of Fluids

Special Topic: Shock Waves

Submit Today!

Thermodynamic analysis of absorption refrigeration cycles by parabolic trough collectors

Cite as: Phys. Fluids **35**, 067118 (2023); doi: [10.1063/5.0153839](https://doi.org/10.1063/5.0153839)

Submitted: 12 April 2023 · Accepted: 30 May 2023 ·

Published Online: 13 June 2023



View Online



Export Citation



CrossMark

Abdullah Albaker,^{1,a)} Nestor Cuba Carbajal,^{2,b)} Manuel Octavio Fernández Athó,^{3,c)} Anderson Nuñez Fernandez,^{4,d)} Maria Del Carmen Delgado Laime,^{3,e)} Ani Mary Borda Echavarría,^{3,f)} Reza Alayi,^{5,b)} and Morteza Aladdin^{6,b)}

AFFILIATIONS

¹Department of Electrical Engineering, College of Engineering, University of Ha'il, Ha'il 81451, Saudi Arabia

²Departamento Académico, Gestión Pública y Gobernabilidad, Universidad Norbert Wiener, Avenida Arequipa 440, Lima, Perú

³Department of Ingeniería Ambiental, Universidad Nacional José María Arguedas, Andahuaylas 03701, Perú

⁴Department of Ingeniería, Universidad Nacional Micaela Bastidas de Apurímac, Abancay, Perú

⁵Department of Mechanical Engineering, Germi Branch, Islamic Azad University, Germi 1477893855, Iran

⁶Department of Mechanics, Kabul University, Afghanistan

^{a)}Electronic mail: af.albaker@uoh.edu.sa

^{b)}Authors to whom correspondence should be addressed: nestor.cuba@uwiener.edu.pe; reza_alayi@iaugermi.ac.ir; and morteza_aladdin@yahoo.com

^{c)}Electronic mail: mfernandez@unajma.edu.pe

^{d)}Electronic mail: anunez@unamba.edu.pe

^{e)}Electronic mail: mcdelgado@unajma.edu.pe

^{f)}Electronic mail: aborda@unajma.edu.pe

ABSTRACT

The purpose of this study is to numerically investigate the performance of a solar physical surface absorption cooling system, in which activated carbon/methanol is used as a working pair, which is placed inside a parabolic-shaped solar collector. The governing mathematical model of this issue is based on the equations of conservation of mass, conservation of energy, and thermodynamics of the physical surface absorption process. The equations are discretized using the fully implicit finite difference method, and the Fortran computer program was simulated. A comparison with the results of previous laboratory and numerical studies validated this model. At each point in the bed, the temperature, pressure, and mass of the refrigerant absorbed during the physical surface absorption/discharge process were calculated. In addition, the effects of the bed diameter, amount of solar radiation, source temperature, temperature, and pressure of the evaporator and condenser were investigated on the solar performance coefficient and the specific cooling power of the system. According to the built laboratory model and the working conditions of the system, the solar performance coefficient and the specific cooling capacity of the system are equal to 0.12 and 45.6 W/kg, respectively.

Published under an exclusive license by AIP Publishing. <https://doi.org/10.1063/5.0153839>

NOMENCLATURE

C_{ps}	Absorbent specific heat	P	Pressure (kPa)
D	Proximity coefficient	Q_c	The heat generated in the evaporator
h_{gl}	Overall heat transfer coefficient	R	The specific constant of the absorbent
$H_g(T)$	Specific enthalpy of methanol in the gas phase	T	Temperature (K)
$H_a(T)$	Specific enthalpy of methanol in the adsorbed phase	T_{ags}	Absorption temperature
L_r	Absorber length	T_{con}	Condenser temperature
n	Characteristic of the absorber/adsorbed pair	T_{ev}	Evaporator temperature
		$T(T_{ev})$	Latent heat of methanol at evaporator temperature (0 °C)

W_O	The total volume of accessible microspores absorbed in the vapor state
x (KgKg^{-1})	Absorbed mass of the refrigerant per unit mass of the absorbent
λ_e	Coefficient of heat transfer of absorbent displacement
ε	The amount of porosity
ρ	Absorbent density

I. INTRODUCTION

Since the time of the Montreal Protocol on the nonuse of chlorofluorocarbons, researchers have started to investigate cooling technologies compatible with the environment and with the feature of not destroying the ozone layer. Physical surface absorption cooling systems are a suitable solution for the pollution problem of these systems. These systems are very important to meet the need for cooling, such as air conditioning, heating, and food and medicine storage in areas without electricity networks. In comparison with vapor compression cooling systems, these systems have many advantages. Vapor condensation refrigeration systems do not cause noise pollution, they usually use environmentally compatible materials as refrigerants (such as water and methanol), they do not have any moving parts, and do not need any other source of energy except solar energy—ammonium, etc.^{1,2} In addition to all the mentioned advantages, these systems have disadvantages in comparison with commercial types of cooling systems, such as high weight and volume, specific cooling capacity, and low performance coefficient.^{3,4} In recent decades, many different types of physical surface absorption cooling systems with different geometries and working pairs have been designed, built, and analyzed. In most of them, activated carbon/ammonium, activated carbon/methanol, silica gel/water, and zeolite/water have been used as adsorption working pairs. These research works are usually carried out in the fields of ice production (ice makers),^{5–7} production of refrigeration for food and drug storage,^{8–10} and air conditioning.^{11,12} Generally, alternating cooling systems with an absorbent bed that can produce cooling only during the night have been studied. Recently, in an experimental study to improve the performance, Hamrahi *et al.*¹³ investigated the effect of activated nano carbon as a part of the absorbent substrate on the performance of the solar surface absorption chiller. Wang *et al.*¹⁴ compared the performance of the solar surface absorption refrigerator with the composite parabolic collector. Fader¹⁵ also introduced a new process to improve the performance of a continuous surface absorption cooling system. The collector/absorber is considered one of the most important parts of these systems, which requires careful investigation. The improvement of physical surface absorption cooling systems is still limited in terms of the cost of building solar absorber collector components.¹⁶ Recently, the high cost of solar collectors has been mentioned as an obstacle to the mass production and commercialization of physical surface absorption cooling systems.¹⁷ Nevertheless, it is possible to reduce the cost of the collector by increasing the performance coefficient of the system or reducing the working temperature of the system.¹⁸ Shape parabolic solar collector has been used as a logical replacement for their previous types. This type of collector increases the efficiency of the system with its high efficiency.¹⁹ Parabolic-shaped collectors are the most advanced and comprehensive solar concentrating collectors based on numerous tests, and their technology is the most approved technology among other types of solar concentrating collectors.²⁰ Liang *et al.*²¹ presented

progress in full spectrum solar energy utilization by the spectral beam splitting hybrid PV/T system. Basdanis *et al.*²² presented a performance optimization of a solar adsorption chiller by dynamically adjusting the half-cycle time. Jahangir *et al.*²³ presented attempts to design and introduce a novel green HVAC system that reduces both energy consumption and carbon production of buildings. This system uses solar absorption chillers to provide the cooling demands of buildings. The system of Roumpedakis *et al.*²⁴ is designed to operate under intermittent heat supply of low-temperature solar thermal energy ($<90^\circ\text{C}$) provided by evacuated tube collectors. The system is designed to operate under an intermittent heat supply of low-temperature solar thermal energy ($<90^\circ\text{C}$) provided by evacuated tube collectors. Jalil and Goudarzi²⁵ simulated an effect of adsorbent configuration on performance enhancement of a continuous solar adsorption chiller with four quadric parabolic concentrators.

According to the research conducted in the field of surface absorption cooling systems and the need to improve their performance, it is still necessary to conduct a study to improve the performance of this type of cooling system. For this purpose, the authors of this study are looking for a two-bed physical surface absorption chiller with maximum efficiency. For this purpose, after designing and building this system, in the second step, it has been optimized with the help of simulation and numerical methods.

In this study, a physical surface absorption chiller with two absorbent beds with a continuous cycle and containing activated carbon/methanol as the absorption working pair (which are placed in a complex parabolic collector) is simulated. In this system, a compound parabolic collector is used for the first time. Also, the effect of absorber bed diameter, amount of solar radiation, cold source temperature, temperature, and pressure (saturation pressure according to temperature) of evaporator and condenser on the solar performance coefficient of the specific cooling power of the system is investigated.

II. MATERIALS AND METHODS

A. System description

Figure 1 shows a view of the continuous physical surface absorption cooling system with two absorption beds. This system includes a parabolic solar collector, a cool water tank, a condenser, a methanol tank, refrigerant valves, and a cylindrical absorption bed containing activated carbon/methanol, etc. Each absorber is located in the focal point of the parabolic solar collector, which includes an inner tube containing a working pair of activated carbon/methanol and an outer tube coaxial with the absorber tube to pass cool water to cool the substrates. During the operation of heating the beds, cold water settles in the outer pipe, and the beds are heated under the direct effect of solar radiation; during the operation of cooling, a protective layer is inadvertently placed on the surface of each solar collector, and the cold water starts moving in the system. To continuously produce cooling, two absorbers work opposite each other. For example, when absorber 1 is preheating and discharging the refrigerant in the condenser under high temperature and pressure (saturation pressure at the temperature of the condenser). Absorber 2 is cooling and absorbs refrigerant at low temperature and pressure (saturation pressure at evaporator temperature). When adsorbent 1 removes methanol, methanol is condensed in the condenser, and then the liquid methanol goes to the evaporator by passing through the control valve. At the same time, absorber 2 is cooled by cold water. As soon as the bed cools down to the

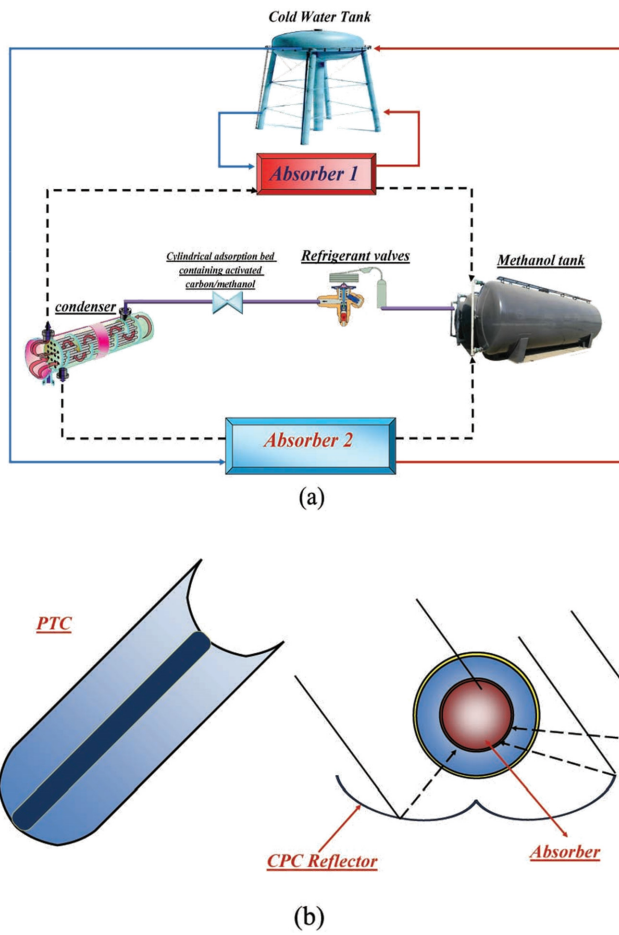


FIG. 1. (a) Absorption refrigeration cycle with parabolic solar collector. (b) Parabolic trough collector.

temperature of the evaporator and reaches its pressure, absorber 2 is connected to the evaporator, and the refrigerant inside the evaporator evaporates. Then, it is absorbed into the bed, and as a result, cooling is achieved in the chamber around it.

B. Numerical modeling

The mathematical model governing the problem is based on the equations of conservation of mass, conservation of energy, and thermodynamics of the physical surface absorption process in the porous medium, discretized by a fully implicit finite difference method and simulated by the Fortran computer program. The desired hypotheses in this simulation are as follows:

1. In each bed, the pressure is assumed to be uniform;
2. The substrate is assumed to be a continuous porous medium;
3. Conductive heat transfer in a porous bed is characterized by a thermal conductivity coefficient equal to λ_a ;
4. The action of physical surface absorption/repulsion is considered a constant pressure;
5. The porous substrate and its properties have axial symmetry;

6. All phases are assumed to be in continuous thermal, mechanical, and chemical equilibrium;
7. Heat transfer is radial, and displacement heat transfer in the radial direction due to mass transfer is ignored;
8. The temperature of the cold source is assumed to be uniform;
9. We assume that the condenser and the evaporator are ideal; therefore, the pressure T_{con} and T are constant in each phase;
10. The gas phase behaves as a complete gas.

C. Mathematical equations of the model

Considering the mentioned hypotheses, a one-dimensional model based on mass and heat transfer and thermodynamics of the adsorption process inside the absorbent bed has been developed. The governing equations include mass and heat transfer equations in the absorbent bed as follows.

The equation for the survival of a crime:

By writing the mass conservation of methanol in a control volume (a layer of m thickness in the radial position r from the cylindrical bed axis)

$$\frac{\partial}{\partial t} [2\pi r dr L_r ((\epsilon - \theta)\rho_g + \theta\rho_a)] = q(r, t) - q(r + dr, t) = -\frac{\partial q}{\partial t} dr, \tag{1}$$

where q is the methanol flow rate in the layers of the adsorbent bed.

1. Energy conservation equation

Similarly, by writing the conservation of energy in a control volume of the absorbent bed^{26,27}

$$\frac{\partial}{\partial t} [2\pi r dr L_r ((1 - \epsilon)\rho_s u_s + (\epsilon - \theta)\rho_g u_g + \theta\rho_a u_a)] + q(r + dr, t)H_g(T(r + dr), P) - q(r, t)H_g(T(r), P) = 2\pi r \lambda_e dr L_r \left[\frac{\partial^2 T}{\partial r^2} + \frac{1}{r} \frac{\partial T}{\partial r} \right], \tag{2}$$

$$H_g(T) = H_a(T) + \Delta H_{ads}, \tag{3}$$

where $H_g(T)$ and $H_a(T)$ are the specific enthalpy of methanol in the gas phase and adsorbed phase, respectively. The latent heat of absorption ΔH_{ads} is calculated using the Clausius-Clapyron equation:²⁶

$$\Delta H_{ads} = RT^2 \left(\frac{\partial \ln P}{\partial T} \right)_x. \tag{4}$$

In this relation, R is the specific constant of the absorbent, x is the absorbed mass of the refrigerant per unit mass of the absorbent (KgKg^{-1}), and it is a function of temperature (T) and pressure (P) of the absorbent bed. This parameter is estimated using the Dobinin-Astakhov (D-A) equation:²⁷

$$X = w_{0\rho_1}(T) \exp \left[-D \left(T \ln \left(\frac{P_{sat}}{P} \right) \right)^n \right], \tag{5}$$

where ρ_1 in this relation is the density of the absorbent in the liquid state and W_0 is the total volume of accessible microspores absorbed in the vapor state; D is the proximity coefficient and n is the characteristic of the absorber/adsorbed pair. For the activated carbon/methanol pair

Downloaded from http://pubs.aip.org/aip/pof/article-pdf/doi/10.1063/5.0153839/1797597/067118_1_5.0153839.pdf

used in this research, the numerical values of D , W_O , and n are $0.425 \times 10^{-3} \text{ m}^3 \text{ Kg}^{-1}$, $5.02 \times 10^{-7} \text{ K}^{-n}$, and 2.15, respectively.²⁸

Combination of mass and heat transfer equations in porous media:

From the combination of mass transfer and heat transfer equations (1) and (2) to the coupling equation of mass and heat transfer, it is obtained as follows:^{27,28}

$$\left[\left((1 - \varepsilon) \rho_s C_{ps} + (\varepsilon - \theta) \rho_g C_{pg} + \theta \rho_a C_{pa} \right) \right] \frac{\partial T}{\partial t} = \lambda_e + \left[\frac{\partial^2 T}{\partial r^2} + \frac{1}{r} \frac{\partial T}{\partial r} \right] + \frac{\partial}{\partial t} \left((\varepsilon - \theta) \rho_g \right) \frac{P}{\rho_g} + \frac{1}{2\pi r dr L_r} \left(\frac{P}{\rho_a} + \Delta H_{ads} \right) \left(\frac{\partial m_a}{\partial t} \right). \tag{6}$$

Initial and boundary conditions

In the following, to complete the mathematical model, the initial and boundary conditions are defined as follows:

Initial conditions²⁶⁻²⁸

$$\begin{aligned} T_1(t = 0) &= T_{min} \\ P_1(t = 0) &= P_{ev} = P_{sat}(T_{ev}) \text{ for absorber (1),} \\ T_2(t = 0) &= T_{max} \\ P_2(t = 0) &= P_{con} = P_{sat}(T_{con}) \text{ for absorber (2).} \end{aligned} \tag{7}$$

The pressure boundary conditions in each absorber whenever they are connected to the evaporator/condenser

$$P(t) = P_{ev/con}. \tag{9}$$

Temperature boundary conditions²⁶

$$r = R_0 : -\lambda_e \left(\frac{\partial T}{\partial r} \right)_{r=R_0} = h_{gl}(T_{HTF} - T) \text{ in absorption,} \tag{10}$$

$$r = R_0 : \lambda_e \left(\frac{\partial T}{\partial r} \right)_{r=R_0} = Irr \text{ in the disposal,} \tag{11}$$

where h_{gl} is the overall heat transfer coefficient between the heat transfer fluid and the absorber bed, and Irr is the amount of solar radiation received in the process of removal by the bed inside the collector, an example of which is shown in Fig. 2.^{29,30} The weather conditions are following the clean days of April in the month of Ardebil. These

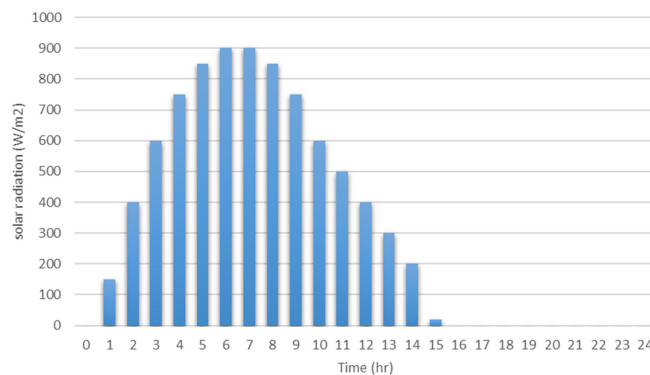


FIG. 2. Amount of solar radiation per unit of the absorbent surface during the d.

weather conditions are shown in Fig. 2, and other input information used in the simulation program is given in Table I.

D. Performance analysis

The performance evaluation characteristics of the solar surface absorption chiller system in this research are solar performance coefficient and specific cooling power. The obtained solar performance coefficient is defined as the ratio between the cooling produced and the solar energy hitting the collector plate during the whole day,

$$COPs = \frac{Q_c}{\int_{sunrise}^{sunset} A_c Irr(t) dt}, \tag{12}$$

where Q_c is the heat generated in the evaporator during the absorption cycle. This characteristic is equal to the latent heat of evaporation of the refrigerant minus the sensible heat of cooling the refrigerant from the condenser temperature to the evaporator temperature,

$$Q_c = m_{AC} \Delta \times \left[L \left(T_{ev} - \int_{T_{ev}}^{T_{con}} C_{pl}(T) dT \right) \right]. \tag{13}$$

The specific cooling power is expressed as the ratio between the produced cooling and the cycle time per unit mass of the absorber,

$$SCP = \frac{Q_c}{t_{cycle} \times m_{AC}}. \tag{14}$$

E. Numerical solution method

To solve the equations of absorbent bed, the finite difference numerical method was used completely implicitly. The discretized equations were solved with the help of a three-dimensional matrix algorithm, and the nonlinear equations were also solved by iteration method. Finally, to simulate the behavior of the surface absorption cooling system, the Fortran computer program was used based on the given mathematical model. Figures 3 and 4 show measured and simulated temperatures for the absorbers.

III. RESULTS

A. Validation

To validate the presented modeling results of mass and energy transfer inside the absorber, the necessary test has been carried out on a

TABLE I. The main input information in the simulation.

Parameter	Value	Unit
L_r	0.7	m
λ_e	0.470	
ε	0.67	...
$T(T_{ev})$	9	kJ kg^{-1}
ρ	500	Kgm^{-3}
C_{ps}	0.85	$\text{kJ kg}^{-1} \text{K}^{-1}$
T_{ags}	297.15	K
T_{con}	303.15	K
T_{ev}	273.15	K

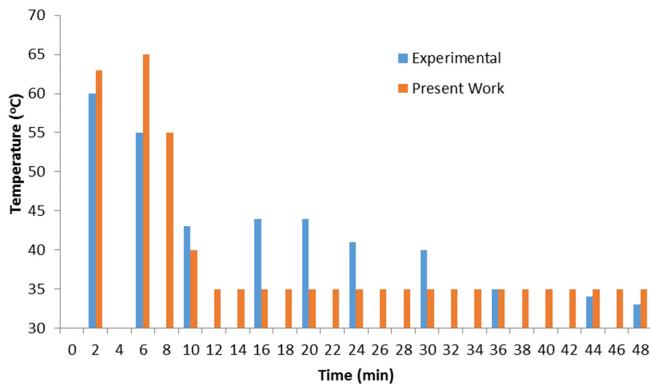


FIG. 3. Measured and simulated temperatures for the absorber 2.

two-bed physical surface absorption cooling system. Each substrate contains a solid cylindrical absorber with a radius of 625.17 mm according to the model made in the laboratory containing 200 gr of activated carbon with the adsorbed working pair of methanol; the starting temperature of the desorption process is 39 °C, and the maximum accessible temperature is 98 °C. Between the hours of 11:30 and 12:30, the simulation day and its results are shown in Figs. 3 and 4, respectively. The experiments were conducted in Ardebil City in February and March (2019).

The complete information on the test device is given in Ref. 13. In Fig. 5 can be seen a geometrical model in the form of two coaxial cylindrical tubes that is insulated from the inner tube of the hot and cold heat transfer fluid and in the space between the two activated carbon tubes with an ammonium working pair and an external wall.¹⁵ It was simulated, and its results are given in Fig. 5. In this form, the temperature changes of the bed during the process of surface physical absorption have been compared in this research and Fadar’s numerical research. As can be seen in the figures, the results obtained from this research have a very good match with the results of the laboratory sample and other references.

B. Modeling results

In this part, the effect of several characteristics on the performance of the system under the working conditions given above is

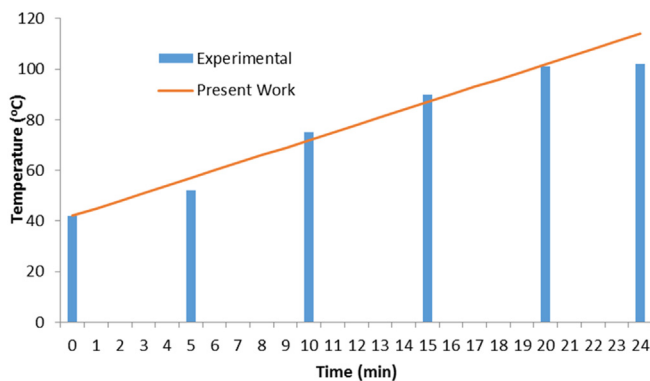


FIG. 4. Measured and simulated temperatures for the absorber 1.

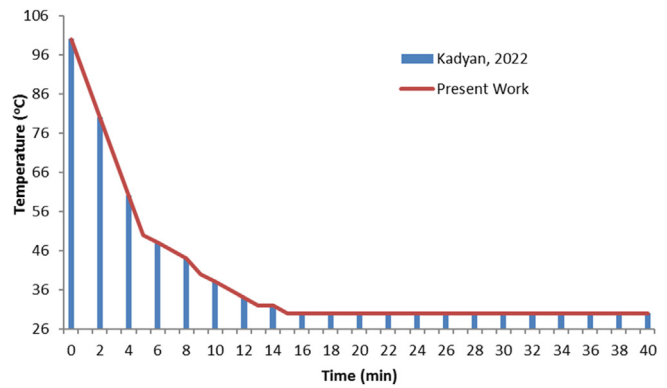


FIG. 5. Kadyan *et al.*¹⁶ and simulated temperatures.

numerically simulated and investigated. The diameter of the absorbent bed, the amount of solar radiation, the temperature of the cold source, and temperature and pressure (saturation pressure according to temperature) of the evaporator and condenser are the investigated characteristics, and the results of which are given in the form of coefficient of performance and specific cooling power in the following figure. Figure 6 shows the temperature changes of the substrate in several different layers in the physical surface absorption and removal processes.

As shown in Fig. 6, i.e., the temperature changes of absorber 2, which is cooling and absorbing physical surface, in the first 20 min, there is an obvious temperature difference between the different layers of the substrate, which shows that the system has not yet reached the absorption equilibrium stage, and then from this time, the system goes through the process of absorption in a balanced way. Absorber 1, which is in the process of preheating and physical surface rejection, can maintain the maximum average temperature of the absorber between all layers due to receiving a continuous heat flux from the sun.

The graph of pressure changes according to the average temperature of the absorber bed between the low-pressure range of the evaporator (saturation pressure corresponding to the temperature of the evaporator) and the high pressure of the condenser (saturation pressure corresponding to the temperature of the condenser) is drawn in

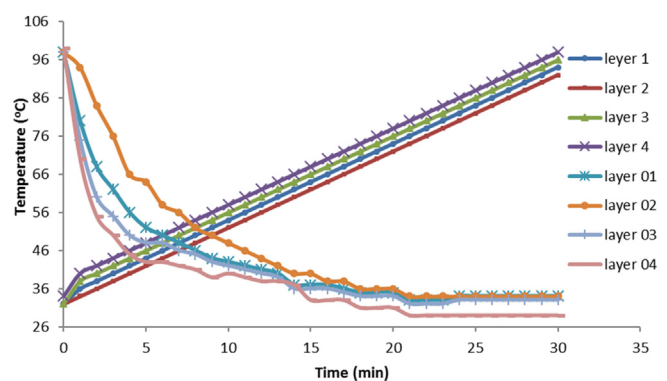


FIG. 6. Simulated temperatures in different layers of each substrate.

Downloaded from http://pubs.aip.org/aip/pof/article-pdf/doi/10.1063/5.0153839/1797597/067118_1_5.0153839.pdf

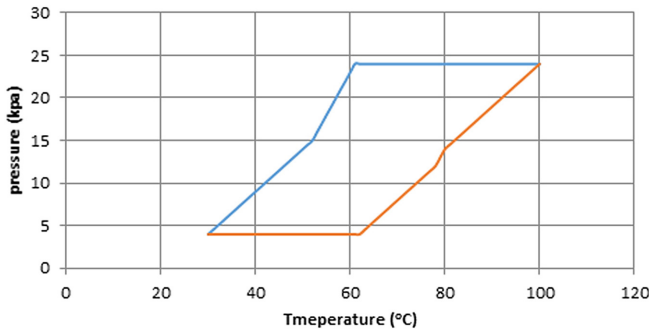


FIG. 7. Simulated bed pressure in the whole cycle.

Fig. 7. In the cooling and preheating part, the refrigerant goes through the process of changing temperature and pressure in a constant mass, the so-called isostatic process, and in the physical surface absorption and repulsion processes, it undergoes a constant pressure (with a changing mass). The changes in absorbed mass in each substrate are shown in Fig. 8. As it is clear from the figure, in the cooling and preheating parts where the temperature and pressure of the refrigerant

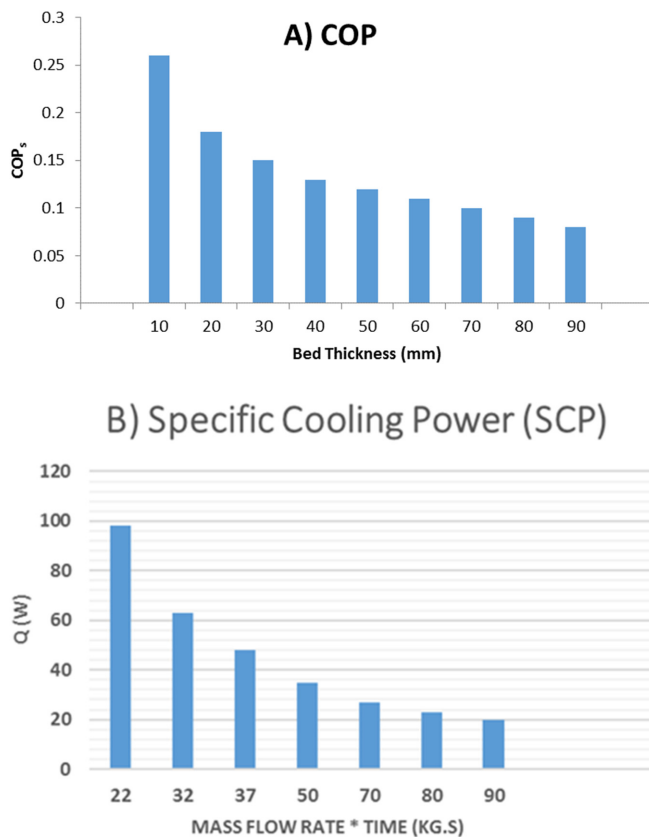


FIG. 8. (a) The amount of refrigerant absorbed in each substrate in the simulation and (b) specific cooling power.

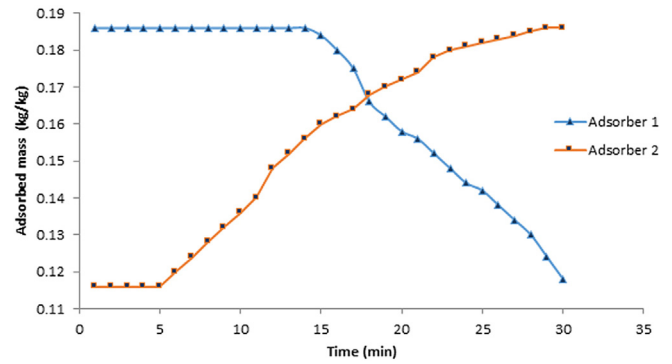


FIG. 9. The effect of bed diameter on solar performance coefficient and special refrigeration power.

change from the evaporator to the condenser or vice versa, the mass is constant, and as soon as the absorption and physical surface removal processes begin, the mass of the refrigerant absorbed per unit mass of the adsorber starts to change. In bed No. 1, because the absorption process is in progress, with time, the amount of absorbed refrigerant mass is increasing at a relatively high rate, and after 20 min, it increases at a lower rate. Also, in bed No. 2, because the disposal process is carried out, the mass of absorbed refrigerant decreases linearly.

The effect of the bed diameter in the working conditions of the evaporator temperature of 29 °C, cold source temperature of 31 °C, and the maximum possible system temperature of 100 °C has been studied. As can be seen in Fig. 9, with the increase in the diameter of the bed, the coefficient of performance and special refrigeration capacity of the system will be reduced. This is due to increasing the period of physical absorption and the surface excretion process, followed by reducing the number of repeating cycles during the duration of sunlight. This will reduce the amount of cooling produced.

Figure 10 shows the effect of solar radiation on two characteristics of the solar performance coefficient and the special refrigeration capability of the system. According to this shape, an increase in the thermal flux will result in a decrease in the solar function coefficient. Due to the increase in thermal flux, the cycle's duration decreases, and therefore, the number of repeated cycle repetitions increases, but the rate of absorbent flux during the day has increased, which ultimately

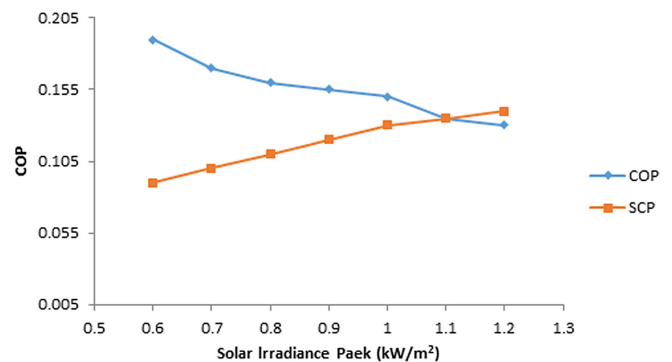


FIG. 10. The effect of solar radiation on the performance coefficient of solar.

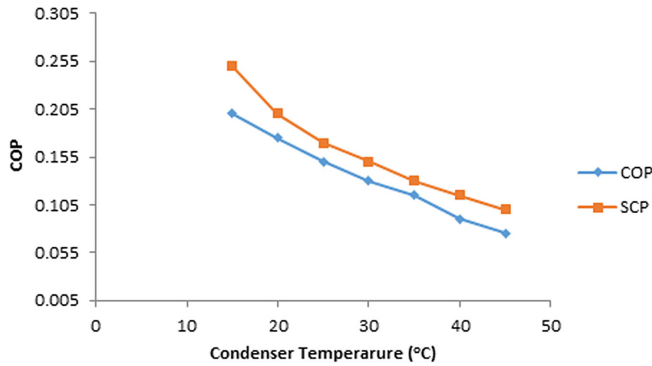


FIG. 11. The effect of cold source temperature on COP and SCP.

results in the effect of the two changes leading to a decrease in solar performance. As mentioned, with the increase in solar thermal flux, the number of repeated cycles increases, and as a result, the number of cooling production increases throughout the day. Therefore, the system's special refrigeration power increases according to Fig. 10.

Reducing the temperature of the cold source leads to an increase in the mass of Δx refrigerant absorption during each process and cycle. On the other hand, the increase in the temperature changes in the system increases the cycle time and reduces the number of repeated cycles during the day. Reducing the temperature of the cold source leads to an increase in the mass of UYY refrigerant absorption during each process and cycle. On the other hand, the increase in the temperature changes in the system increases the cycle time and reduces the number of repeated cycles during the day. According to Fig. 11, the effect of Δx increase is greater, and the solar performance coefficient and special refrigeration capability increase.

Figures 12 and 13 have shown changes in the solar function coefficient and the system's special refrigeration capability in terms of temperature and pressure changes of the evaporator and the condenser. With the increase in temperature and pressure of the evaporator as well as the condenser's temperature and pressure, the solar performance coefficient and the system's special refrigeration strength increase. This is due to the decrease in the tangible heat absorption and easier the refrigerant evaporation process within the evaporator.

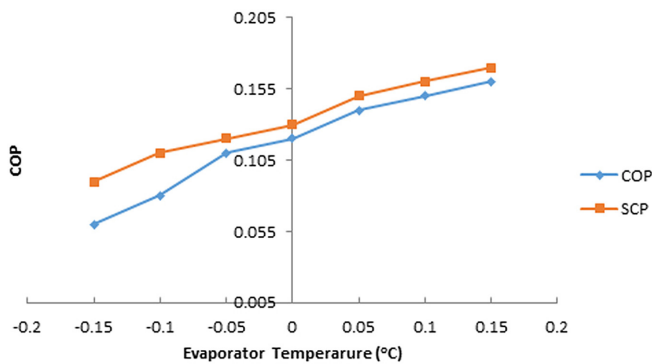


FIG. 12. Effects of the evaporator on performance coefficient of solar.

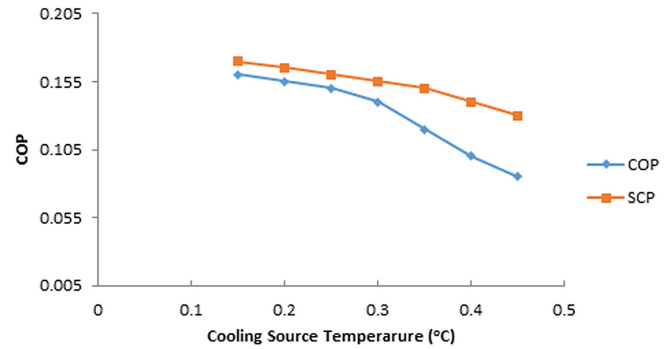


FIG. 13. The effect of the condenser's temperature on the performance coefficient of solar.

Also, with the increasing temperature and pressure of the condenser and the removal of the evaporator temperature and pressure, the solar performance coefficient and the special refrigeration power of the system decrease. The reason is the increased heat of the absorption. As a result, the interval of the absorbed refrigerant mass decreases, and therefore, less cooling is produced.

C. Comparison of results with previous literature

For believability and validation, the obtained results from the current research were compared with the reported results in similar literature. Table II summarizes the comparison of the results. In this regard, Solmuş⁸ developed the balance adsorption capacity of water on a natural zeolite at several zeolite temperatures. He also investigated a transient local thermal non-equilibrium model to evaluate the dynamic heat and mass transfer performance of the absorption cooling cycle. The results indicated that the maximum absorption capacity and values of COP and SCP were almost 0.12, 0.25, and 7 W/kg, respectively. In addition, Bujok *et al.*²⁰ evaluated the possibilities of employing solar collectors (Kingspan Thermomax collector) to power a two-bed adsorption chiller under the climatic conditions of Poland considering the issues related to the integration of all system units. They reported that the value of COP and cooling capacity were 0.531–0.692 and 5.16–8.71 kW, respectively.

Basdanis *et al.*²² developed the simulation of a solar thermal system coupled with the adsorption chiller in real-time investigating the constant and adjusted half-cycle time scenarios. The performance of the solar thermal adsorption chiller was also parameterized. They found that the maximum daily cooling capacity was further increased with adjusted half-cycle time. Moreover, the maximum daily cooling

TABLE II. Comparison of results with previous literature.

Literature	COP	Cooling capacity
Solmuş ⁸	0.25	7 W/kg
Bujok <i>et al.</i> ²⁰	0.531–0.692	5.16–8.71 kW
Basdanis <i>et al.</i> ²²	0.397	18.05 kW
Hamrahi <i>et al.</i> ¹³	0.134	86 W/kg
Current article	0.705	9.21 kW

Downloaded from http://pubs.aip.org/aip/pof/article-pdf/doi/10.1063/5.0153839/1797597/067118_1_5.0153839.pdf

capacity and COP value were equal to 18.05 kW and 0.397, respectively. Hamrahi *et al.*¹³ examined the performance of a solar energy-driven continuous adsorption chiller based on micro- and nano-activated carbon/methanol fluids to improve the COP of solar adsorption chiller. They reported that adding nano-activated carbon could improve chiller performance by up to 33%. In addition to that, the average COP and SCP for water with 34 °C (at 90 g of nano added to the adsorbent bed) were 0.134 and 86 W/kg, respectively. We found in the present article that the highest temperature absorbed by the studied system was 98 °C in the fourth layer. Moreover, for a mass flow rate of 22 kg/s, the amount of heat produced for cooling was 99 W. Furthermore, the values of COP and SCP of the developed system were 0.705 and 9.21 kW, respectively. The performance of the proposed energy system is effectively improved compared to similar systems. Therefore, the developed system can be competitive with the energy systems reported in the literature.

IV. CONCLUSIONS

In this research, to optimize and improve the performance of a two-context-connected superficial recruitment system connected to the solar and continuous cycle collector, the simulation of a numerical code by a computer program for review, analysis, and optimization of the synthesis was performed. The results of the impact of the traits are illuminated by several issues. The high-efficiency solar collector enhances the coefficient of performance and the special refrigeration system of the physical absorption system with a continuous cycle of up to 0.20 and 98. In the lower thickness of the substrate, the coefficient of performance and the special refrigeration power of the system are a significant amount of higher thicknesses. Increasing the amount of solar radiation with the constant maximum possible temperature of the system, despite the rational decrease in the system's solar performance coefficient, increases the system's special refrigeration and cooling rate to double. Suggestion for future work:

Thermo-Economic Analysis for solar absorption chillers.

Energetic and Performance Optimization Absorption Chiller Powered by Parabolic Trough Collector.

Energy and Exergy and Environmental Analysis Absorption Chiller Powered by Parabolic Trough Collector.

AUTHOR DECLARATIONS

Conflict of Interest

The authors have no conflicts to disclose.

Author Contributions

Abdullah Albaker: Conceptualization (equal); Data curation (equal); Formal analysis (equal); Investigation (equal); Methodology (equal). **Nestor Cuba Carbajal:** Conceptualization (equal); Data curation (equal); Formal analysis (equal); Project administration (equal); Validation (equal); Visualization (equal); Writing – original draft (equal); Writing – review & editing (equal). **Manuel Octavio Fernández Athó:** Conceptualization (equal); Formal analysis (equal); Investigation (equal); Methodology (equal). **Anderson Nuñez Fernandez:** Data curation (equal); Formal analysis (equal); Resources (equal); Software (equal); Validation (equal); Visualization (equal). **Maria Del Carmen Delgado Laime:** Conceptualization (equal); Data curation (equal); Validation (equal); Visualization (equal); Writing – original draft (equal); Writing – review & editing (equal). **Ani Mary**

Borda Echavarría: Conceptualization (equal); Data curation (equal); Formal analysis (equal); Validation (equal); Visualization (equal); Writing – original draft (equal); Writing – review & editing (equal). **Reza Alayi:** Conceptualization (equal); Data curation (equal); Formal analysis (equal); Investigation (equal); Writing – original draft (equal); Writing – review & editing (equal). **Morteza Aladdin:** Conceptualization (equal); Funding acquisition (equal); Investigation (equal); Methodology (equal); Project administration (equal); Software (equal); Supervision (equal); Validation (equal); Writing – original draft (equal); Writing – review & editing (equal).

DATA AVAILABILITY

The data that support the findings of this study are included in this article.

REFERENCES

- R. Alayi, N. Khalilpoor, S. Heshmati, A. Najafi, and A. Issakhov, "Thermal and environmental analysis solar water heater system for residential buildings," *Int. J. Photoenergy* **2021**, 6838138.
- R. Alayi, M. Jahangiri, and A. Najafi, "Energy analysis of vacuum tube collector system to supply the required heat gas pressure reduction station," *Int. J. Low-Carbon Technol.* **16**(4), 1391–1396 (2021).
- R. A. Almasri, N. H. Abu-Hamdeh, K. K. Esmail, and S. Suyambazhahan, "Thermal solar sorption cooling systems—A review of principle, technology, and applications," *Alexandria Eng. J.* **61**(1), 367–402 (2022).
- A. A. Hasan, A. Juaidi, R. Abdullah, T. Salameh, O. Ayadi, M. Jaradat, R. E. Hammad, P. E. Campana, and O. A. Aqel, "A review of solar thermal cooling technologies in selected Middle East and North African countries," *Sustainable Energy Technol. Assess.* **54**, 102871 (2022).
- E. M. Nyang'au and K. Kiriamiti, "Solar adsorption cooling with focus on using steatite adsorbent: A review," in *Advances in Phytochemistry, Textile and Renewable Energy Research for Industrial Growth* (CRC Press, 2022), p. 265.
- N. Modi and B. Pandya, "Integration of evacuated solar collectors with an adsorptive ice maker for hot climate region," *Energy Built Environ.* **3**(2), 181–189 (2022).
- N. A. Qasem, "Techno-economic evaluation of novel absorption refrigerator-driven membrane distillation plants," *Energy Convers. Manage.* **270**, 116192 (2022).
- I. Solmus, see <https://hdl.handle.net/11511/21228> for "An experimental study on the performance of an adsorption cooling system and the numerical analysis of its adsorbent bed" (2011).
- X. Hao, S. Shan, N. Gao, G. Chen, Q. Wang, and T. Gu, "Performance analysis of a novel combined cooling, heating and power system with solar energy spectral beam splitting," *Energy Convers. Manage.* **276**, 116500 (2023).
- S. Chu, H. Zhang, and H. Chen, "Energy, exergy, energy-saving, economic and environmental analysis of a micro-gas turbine-PV/T combined cooling, heating and power (CCHP) system under different operation strategies: Transient simulation," *Energy Convers. Manage.* **276**, 116557 (2023).
- K. M. Almohammadi and K. Harby, "Operational conditions optimization of a proposed solar-powered adsorption cooling system: Experimental, modeling, and optimization algorithm techniques," *Energy* **206**, 118007 (2020).
- T. Salameh, A. Alkhalidi, M. K. H. Rabaia, Y. Al Swailmeen, W. Alroujmah, M. Ibrahim, and M. A. Abdelkareem, "Optimization and life cycle analysis of solar-powered absorption chiller designed for a small house in the United Arab Emirates using evacuated tube technology," *Renewable Energy* **198**, 200–212 (2022).
- S. Hamrahi, K. Goudarzi, and M. Yaghoubib, "Experimental study of the performance of a continues solar adsorption chiller using nano-activated carbon/methanol as working pair," *Sol. Energy* **173**, 920–927 (2018).
- Y. Wang, M. Li, W. Du, Q. Yu, X. Ji, and X. Ma, "Performance comparative study of a solar-powered adsorption refrigerator with a CPC collector/adsorbent bed," *Energy Convers. Manage.* **173**, 499–507 (2018).
- A. E. Fader, "Novel process for performance enhancement of a solar continuous adsorption cooling system," *Energy* **114**, 10–23 (2016).

- ¹⁶H. Kadyan, A. K. Berwal, and R. S. Mishra, "A novel intelligent strategy--based thermodynamic modeling and analysis of solar-assisted vapor absorption refrigeration system," *Environ. Sci. Pollut. Res.* **29**, 71518–71533 (2022).
- ¹⁷S. A. Mousavi, M. Mehrpooya, and M. Delpisheh, "Development and life cycle assessment of a novel solar-based cogeneration configuration comprised of diffusion-absorption refrigeration and organic Rankine cycle in remote areas," *Process Saf. Environ. Prot.* **159**, 1019–1038 (2022).
- ¹⁸M. Dannemand, I. Sifnaios, Z. Tian, and S. Furbo, "Simulation and optimization of a hybrid unglazed solar photovoltaic-thermal collector and heat pump system with two storage tanks," *Energy Convers. Manage.* **206**, 112429 (2020).
- ¹⁹N. Abed, I. Afgan, H. Iacovides, A. Cioncolini, I. Khurshid, and A. Nasser, "Thermal-hydraulic analysis of parabolic trough collectors using straight conical strip inserts with nanofluids," *Nanomaterials* **11**(4), 853 (2021).
- ²⁰T. Bujok, M. Sowa, P. Boruta, Ł. Mika, K. Sztékler, and P. R. Chaja, "Possibilities of integrating adsorption chiller with solar collectors for polish climate zone," *Energies* **15**(17), 6233 (2022).
- ²¹H. Liang, F. Wang, L. Yang, Z. Cheng, Y. Shuai, and H. Tan, "Progress in full spectrum solar energy utilization by spectral beam splitting hybrid PV/T system," *Renewable Sustainable Energy Rev.* **141**, 110785 (2021).
- ²²T. Basdanis, A. Tsimpoukis, and D. Valougeorgis, "Performance optimization of a solar adsorption chiller by dynamically adjusting the half-cycle time," *Renewable Energy* **164**, 362–374 (2021).
- ²³M. H. Jahangir, A. Kargarzadeh, and F. Javanshir, "Energy investigation in buildings applying a solar adsorption chiller coupled with biofuel heaters and solar heating/cooling systems in different climates," *Energy Rep.* **8**, 15493–15510 (2022).
- ²⁴T. C. Roumpedakis, S. Vasta, A. Sapienza, G. Kallis, S. Karellas, U. Wittstadt, M. Tanne, N. Harborth, and U. Sonnenfeld, "Performance results of a solar adsorption cooling and heating unit," *Energies* **13**(7), 1630 (2020).
- ²⁵E. Jalil and K. Goudarzi, "Effect of adsorbent configuration on performance enhancement of continuous solar adsorption chiller with four quadric parabolic concentrators," *Renewable Energy* **158**, 360–369 (2020).
- ²⁶S. W. Hong, S. H. Ahn, O. K. Kwon, and J. D. Chung, "Optimization of a fin-tube type adsorption chiller by design of experiment," *Int. J. Refrig.* **49**, 49–56 (2015).
- ²⁷W. Chekirou, N. Boukheit, and A. Karaali, "Heat recovery process in an adsorption refrigeration machine," *Int. J. Hydrogen Energy* **41**(17), 7146–7157 (2016).
- ²⁸Y. Teng, R. Z. J. Wang, and Y. Wu, "Study of the fundamentals of adsorption systems," *Appl. Therm. Eng.* **17**(4), 327–338 (1997).
- ²⁹M. M. Dubinin and V. A. Astakhov, *Development of the Concept of Volume Filling of Micropores in the Adsorption of Gases and Vapors by Microporous Adsorbents* (American Chemical Society, Washington DC, 1971).
- ³⁰M. Aramesh, F. Pourfayaz, M. Haghiri, A. Kasaieian, and M. H. Ahmadi, "Investigating the effect of using nanofluids on the performance of a double-effect absorption refrigeration cycle combined with a solar collector," *Proc. Inst. Mech. Eng., Part A* **234**(7), 981–993 (2020).